JOURNAL OF THERMOPHYSICS AND HEAT TRANSFER
Vol. 24, No. 4, October–December 2010

# Technical Notes

## Boundary Heat Fluxes in a Square Enclosure with an Embedded Design Element

M. Ajith,* Ranjan Das,† Ramagopal Uppaluri,‡ and Subhash C. Mishra†
*Indian Institute of Technology, Guwahati, Assam 781 039, India*

DOI: 10.2514/1.49910

### Nomenclature

| | | |
|---|---|---|
| $C_p$ | = | specific heat, $\frac{\text{kJ}}{\text{kgK}}$ |
| $\mathbf{c}_i^*$ | = | nondimensional propagation velocity, $(\frac{\Delta \mathbf{r}^*}{\Delta \xi})$ |
| $f_i^*$ | = | nondimensional particle distribution function in the $i$ direction |
| $f_i^{*0}$ | = | nondimensional equilibrium particle distribution function in the $i$ direction |
| $G$ | = | incident radiation, $\frac{\text{kW}}{\text{m}^2}$ |
| $J$ | = | nondimensional fitness function |
| $k$ | = | thermal conductivity, $\frac{\text{kW}}{\text{mK}}$ |
| $N$ | = | conduction-radiation parameter, $\frac{k\beta}{4\sigma T_{\text{ref}}^3}$ |
| $n$ | = | number of lattices, equal to 20 |
| $q$ | = | heat flux, $\frac{\text{kW}}{\text{m}^2}$ |
| $\mathbf{r}^*$ | = | nondimensional distance along $x$ and $y$ coordinates of the lattice, $\frac{r}{x\,\text{max}}$ |
| $\Delta \mathbf{r}^*$ | = | $\mathbf{r}^*/n$ |
| $r$ | = | distance along $x$ and $y$ coordinates of the lattice, m |
| $T$ | = | temperature, K |
| $t$ | = | time, s |
| $w$ | = | weights of particle in the lattice |
| $\Delta x$ | = | elemental distance in $x$-direction, m |
| $X$ | = | distance along $x$-axis, m |
| $x$ max | = | maximum distance in $x$-direction, m |
| $x$ min | = | minimum distance in $x$-direction, m |
| $y$ max | = | maximum distance in $y$-direction, m |
| $y$ min | = | minimum distance in $y$-direction, m |
| $Y$ | = | distance along $y$-axis, m |
| $\alpha$ | = | thermal diffusivity, $\frac{\text{m}^2}{\text{s}}$ |
| $\beta$ | = | extinction coefficient, $\frac{1}{\text{m}}$ |
| $\Delta \xi$ | = | elemental nondimensional time, $\alpha \beta^2 \Delta t$ |
| $\delta$ | = | polar angle, rad |
| $\varepsilon$ | = | emissivity |
| $\xi$ | = | nondimensional time, $\alpha \beta^2 t$ |
| $\rho$ | = | density, $\frac{\text{kg}}{\text{m}^3}$ |
| $\sigma$ | = | Stefan–Boltzmann constant, $\frac{\text{kW}}{\text{m}^2\text{K}^4}$ |
| $\sigma_s$ | = | scattering coefficient, $\frac{1}{\text{m}}$ |
| $\tau^*$ | = | nondimensional relaxation time, $\frac{3}{\lvert \mathbf{c}_i^* \rvert^2} + \frac{\Delta \xi}{2}$ |
| $\Psi_R$ | = | nondimensional radiative heat flux, $(\frac{q_R}{\sigma T^4/\pi})$ |
| $\omega$ | = | scattering albedo $(\sigma_s/\beta)$ |

*Subscripts*

| | | |
|---|---|---|
| 1, 2 | = | hot and cold boundaries |
| $b$ | = | boundary |
| $C$ | = | conductive |
| design | = | design surface |
| $e$ | = | east |
| heater | = | heater surface |
| $i$ | = | $x$-direction in the lattice |
| $j$ | = | $y$-direction in the lattice |
| maximum | = | maximum heat flux |
| mean | = | average heat flux |
| $n$ | = | north |
| $R$ | = | radiative |
| ref | = | reference |
| $s$ | = | south |
| uniform | = | uniform heat flux |
| $w$ | = | west |

*Superscripts*

| | | |
|---|---|---|
| $*$ | = | nondimensional |
| $k$ | = | index for time step |

Received 17 March 2010; revision received 1 August 2010; accepted for publication 2 August 2010. 

*Department of Chemical Engineering; ramgopalu@iitg.ernet.in.
†Department of Mechanical Engineering.
‡Department of Chemical Engineering (Corresponding Author).

### I. Introduction

THE thermal analysis of many devices such as furnaces, ovens and infrared heating chambers involve thermal radiation [1] as the dominant mode of heat transfer and they invariably require the determination of temperature or heat flux distribution which may involve conduction in conjunction with radiation. The geometry in real time industrial applications is unlike a typical 2-D enclosure [2], due to the fact that it contains a sample embedded inside an enclosure. Analysis of such a system with mixed boundary conditions (where flux is provided and temperature distributions are sought or vice–versa) and inverse formulation are essential. Problems of such type require solution of the energy equation involving conduction and radiation [3,4].

The present work adopts a lattice Boltzmann method (LBM) [5], finite volume method (FVM) [6], and genetic algorithm (GA) [7] approach to study the effect of modeling tools for the design of high temperature heater enclosures in a 2-D geometry. This work attempts to target the modeling study to develop general guidelines towards the design of high temperature heaters. Further, the optimization of the sample positioning in the heater is also addressed in this article. The next section outlines the formulation and results pertaining to the analysis in a 2-D geometry.

### II. Formulation

The geometry considered in the present work is shown in Fig. 1. The enclosure constitutes an absorbing, emitting and isotropically scattering medium with diffuse gray boundaries. Initially the system is at temperature $T_2$. For time $t > 0$, the heater surface is raised to temperature $T_1$ and the design surface is at a constant temperature of $T_{\text{design}}$. at steady state. The thermophysical and optical properties of the medium (Fig. 1) are constant and the heat flux is calculated on the design surface. Subject to these boundary conditions, the energy equation is solved in the medium using LBM, and the radiative information is evaluated using FVM. In the absence of convection and heat generation, for a homogeneous medium, the energy

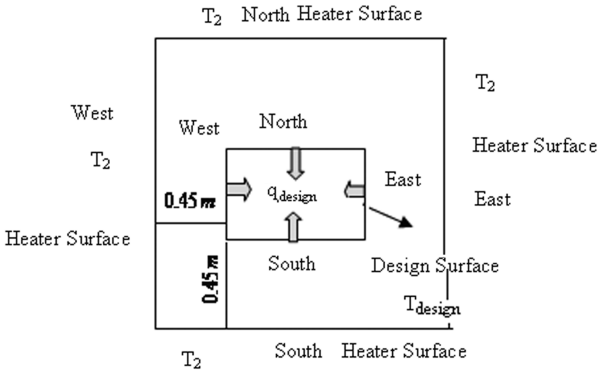


**Fig. 1 Schematic of 2-D heater with sample embedded in it.**

equation is given by

$$\rho C_p \frac{\partial T}{\partial t} = k\nabla^2 T - \nabla \cdot \mathbf{q}_R \tag{1}$$

where

$$\nabla.\mathbf{q}_R = \beta(1-\omega)\left(4\pi\frac{\sigma T^4}{\pi} - G\right) \tag{2}$$

The details about various terms in Eqs. (1) and (2) can be found in [6,8–12]. The method of solution of the energy equation [Eq. (1)] and subsequent determination of temperature distribution using the LBM–FVM methodology has been described in the literature [6,8–12]. Therefore, it is not reproduced here. The nondimensional final form of the energy equation in LBM is written as

$$f_i^*(\mathbf{r}^* + \mathbf{c}_i^*\Delta\xi, \xi + \Delta\xi) = f_i^*(\mathbf{r}^*, \xi) - \frac{\Delta\xi}{\tau^*}[f_i(\mathbf{r}^*, \xi) - f_i^{*0}(\mathbf{r}^*, \xi)] - \frac{\Delta\xi w_i}{4N}\nabla \cdot \Psi_R \tag{3}$$

In Eq. (3), $\mathbf{r}^*$, $\tau^*$, and $\mathbf{c}_i^*$ are the location, the relaxation time, and the particle velocity, respectively, in nondimensional form as defined in the nomenclature. The details about all terms in Eq. (3) have been described in [8–12]. Using an inverse approach, below we discuss the method of obtaining the minimum/optimal heat flux at one of the boundaries (heater surface), which would yield a given heat flux distribution at the other boundary (design surface). For the minimization of the objective function involving the heat flux at the heater surface, we have used the GA. The two objective functions considered for the analysis are given below

$$(J)_{\text{uniform}} = \frac{1}{\{\sum_{i=x\min}^{x\max}(q_{s,i,\text{design}} - q_{n,i,\text{design}}) + \sum_{j=y\min}^{y\max}(q_{e,i,\text{design}} - q_{w,i,\text{design}})\}} \tag{4}$$

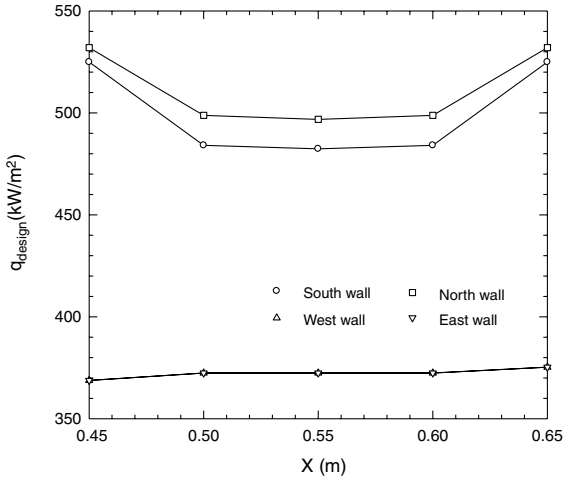


a)

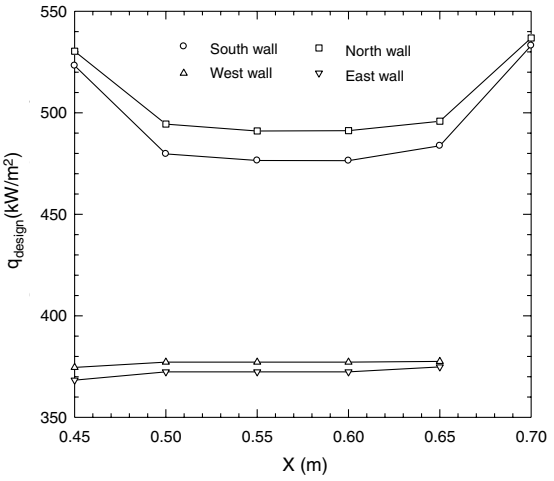


b)

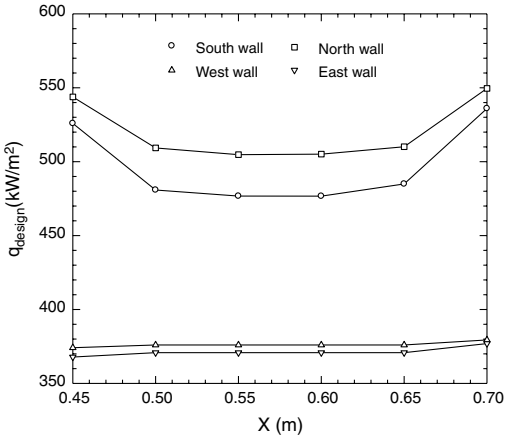


c)

**Fig. 2 Flux distribution along the design surface on the sample: a) 0.20 m × 0.20 m, b) 0.25 m × 0.25 m, and c) 0.25 m × 0.25 m.**

$$(J)_{\text{maximum}} = \left\{ \sum_{i=x\,\min}^{x\,\max} [(q_{s,i,\text{design}} - q_{\text{mean}})^2 + (q_{n,i,\text{design}} - q_{\text{mean}})^2] + \sum_{j=y\,\min}^{y\,\max} [(q_{e,j,\text{design}} - q_{\text{mean}})^2 + (q_{n,j,\text{design}} - q_{\text{mean}})^2] \right\} \quad (5)$$

In the above expressions, Eq. (4) corresponds to the fitness function so as to maximize the total heat flux on the design surface. However, Eq. (5) corresponds to the fitness function referring to the achievement of uniform flux on the design surface. Initially, the position of the design surface is arbitrarily assumed and the flux on the design surface is calculated by solving the system of equations using an iterative approach that encompasses convergence criteria for incident radiation and steady state temperature on the design surface. The convergence criteria for the present work, is reached when it is observed that there is no significant change in the value of the objective functions after a certain number of iterations/generations. The minimum value of the objective function for this convergence was set to $1.0 \times 10^{-6}$. Eventually, the heat flux on every node of the design surface is evaluated using the following equations:

$$q_{\text{design}} = q_R + q_C \quad (6)$$

$$q_{i,C} = \rho C_p (T_{i,j}^{k+1} - T_{i,j}^{k}) \frac{\Delta x}{2} \quad (7)$$

For optimization purposes, in the present work, we have used the GA. The mutation and the crossover probabilities are taken as 0.01 and 0.80 with a two point crossover function and uniform mutation approach. The size of the population and generation parameters in the GA are chosen as 100 and 20, respectively. The model is validated similarly to those presented elsewhere [6,8].

## III. Results and Discussion

In this section, we present the results obtained for few case studies that were chosen to evaluate the effect of various parameters such as design surface dimensions and position on flux-temperature relationships. Further, position optimality to achieve uniform or maximum heat flux is also presented. For all case studies, the heater walls and design sample are kept at a temperature of 2300 and 1150 K, respectively. The medium properties such as the wall emissivity, the scattering albedo, the extinction coefficient and the conduction-radiation parameter selected are $\varepsilon = 1$, $\omega = 0.5$, $\beta = 0.5$, $N = 0.1$, respectively. The size of the heater is taken as 1 m × 1 m. The sizes of the sample are chosen as 0.20 m × 0.20 m; 0.25 m × 0.25 m and 0.25 m × 0.20 m.

### A. Effect of Sample Dimensions on Design Surface Heat Flux

The case study involves evaluation of design surface flux distributions for samples of three different sizes namely 0.2 m× 0.2 m; 0.25 m × 0.25 m and 0.25 m × 0.2 m. For all samples, the sample position is 0.45 m from the south and 0–45 m from the west boundary (Fig. 1). Figures 2a–2c presents the flux distribution along the design surface for the three different samples. It can be observed that a similar heat flux distribution occurs even for different sizes of the sample. In addition to that, it is also observed that the temperature variation is significant along the south and the north walls, and approximately uniform temperature is along the east and the west walls. For the sample size of 0.20 m × 0.20 m, the design surface fluxes are found to be about 482–524, 496–531, 368–375, and

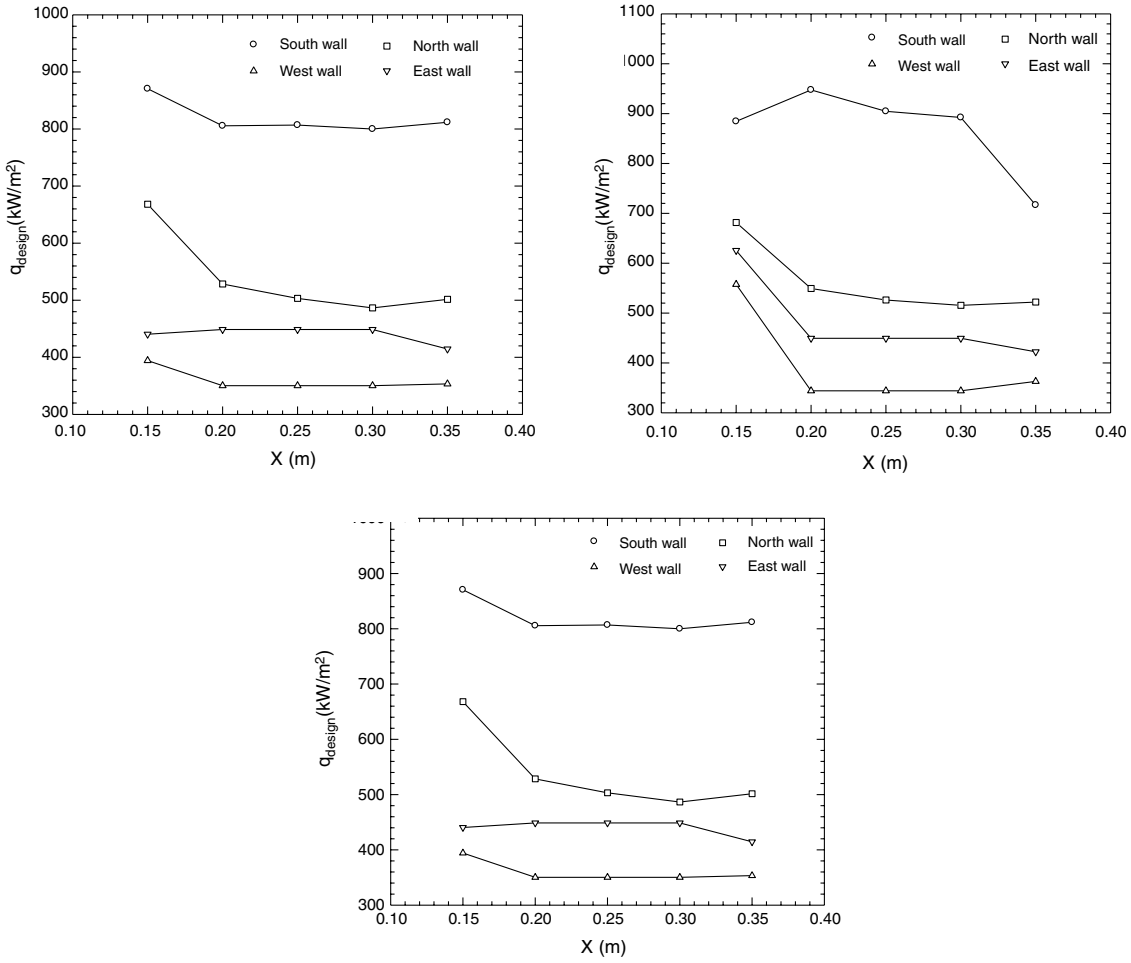


**Fig. 3 Flux distribution on the design surface of the sample for a 0.20 m × 0.20 m sample positioned at a) 0.15 m from south and 0.15 m from west, b) 0.15 m from south and 0.45 m from west, and c) 0.45 m from south and 0.45 m from west boundaries of heater.**

369–375 kW/m$^2$ on the south, north, west, and east walls of the design sample, respectively. However, when the sample size increased to 0.25 m × 0.25 m, the design surface heat fluxes are found to vary about 476–533, 491–536, 374–377, 368–374 kW/m$^2$ for south, north, west and east walls of the design sample, respectively. Also, for the sample size of 0.25 m × 0.20 m, the design surface heat fluxes are found to vary about 476–535, 504–549, 374–379, 370–376 kW/m$^2$ for south, north, west, and east walls of the design sample, respectively.

### B. Effect of Sample Position on Design Surface Heat Flux

For these cases, with orientation of the heater and the sample fixed, the position of the sample is varied. In Figs. 3a–3c three different cases are considered to evaluate the effect of sample position on design surface heat flux. The cases correspond to sample placement 0.15 m from west and 0.15 m from south boundary (case a), 0.15 m from south and 0.45 m from west boundary (case b) and 0.45 m from both east and west boundaries (case c) for a default sample size of 0.20 m × 0.20 m. For case a, the design surface flux distributions are about 799–870, 486–668, 350–394, 414–448 kW/m$^2$ for south, north, east, and west boundaries, respectively. For case b, the design surface flux distributions are about 716–947, 515–681, 344–557, and 422–625 kW/m$^2$ for south, north, east, and west boundaries, respectively. For case c, the design surface flux distributions are about 799–870, 486–668, 350–394, and 414–448 kW/m$^2$ for south, north, east, and west boundaries, respectively. Also, it can be observed that the flux distribution trends associated with the south wall are different for case b in contrast to cases a and c. This is due to the symmetric positioning of the sample in cases a and c but not in case b. In other words, the sample position is a more critical parameter than sample size, due to the high degree of nonuniformity in the heat flux distribution.

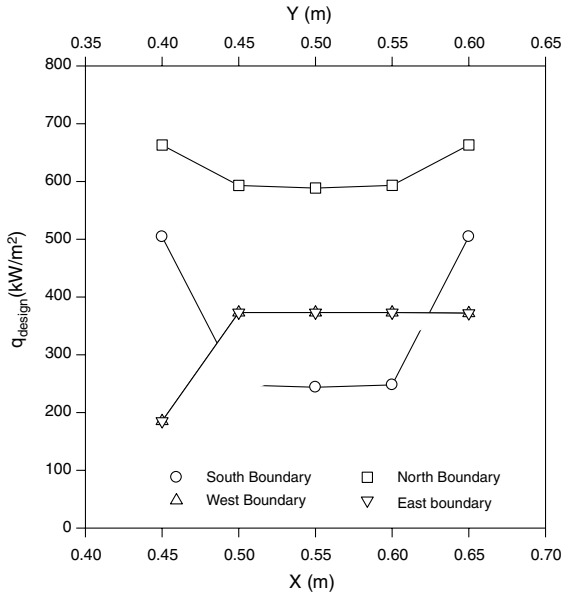


a)

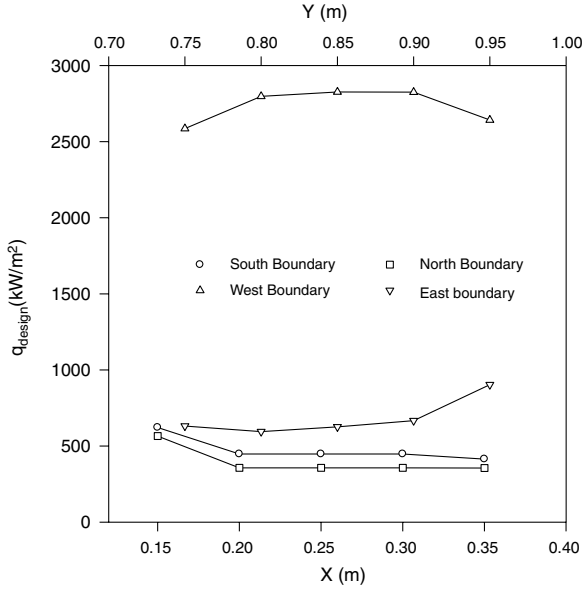


b)

**Fig. 4 Heat flux on the sample for the optimal positioning of the sample: a) to attain minimum deviation from mean flux on sample, and b) to attain maximum flux on sample.**

### C. Optimization of the Heater Position for Uniform and Maximum Heat Distribution on the Sample

Using Eq. (4) as the optimization function, the optimization of heater position to achieve uniform heat flux distribution on the sample is carried out. In the GA, about 10 generations were found to be suitable to achieve solutions that could indicate confidence because the variation after approximately 10 generations was negligible ($\leq 1.0 \times 10^{-6}$). The sample coordinates (0.45, 0.40), (0.65, 0.40), (0.45, 0.60) and (0.65, 0.60) correspond to the optimum location of the sample. Figure 4a presents the variation of heat flux distributions along the design surfaces at this optimum location. It is observed that the heat flux distributions varied about 243–504, 588–663, 184–373 and 184–373 kW/m$^2$ for the south, north, east and west boundary walls, respectively.

Using Eq. (5) as the objective function, the optimization of heater position to achieve maximum heat flux distribution over the sample is carried out. In this case too, about 10 generations were found to be suitable to achieve solutions that could indicate confidence. Four possible global solutions are identified that could provide maximum surface heat flux. As the possibility of having a maximum heat flux is at one of the corners and as the selected geometry has four corners, hence there exist four global solutions using the coordinates (0.15, 0.75), (0.35, 0.75), (0.15, 0.95) and (0.35, 0.95). Figure 4b presents the variation of heat flux distributions along the design surfaces for the first solution wherein the heat flux distributions vary from 414–622, 355–565, 2585–2826 and 594–903 kW/m$^2$ for south, north, east, and west boundary walls, respectively. Therefore, it is apparent that, for a nonuniform heat distribution or an irregular geometry, this work could serve as a potential tool to guide design specifications relating to a single unique solution of the position vector.

## IV. Conclusions

This work addressed an inverse mathematical formulation based solution methodology that can be used to develop relationships between heater surface flux/temperature, design surface temperature/flux and medium properties. LBM-FVM-GA was used as the modeling tool to address design-related issues for the 2-D heater enclosure problem. The study described in this work indicated the existence of various possible solutions due to interdependency of the two modes of heat transfer, viz., conduction and radiation. To have the desired thermal conditions on a design surface, this work provides a general guideline for the selection of heater, medium and material properties.

## References

[1] Modest, M. F., *Radiative Heat Transfer*, 2nd ed., Academic Press, New York, 2003.

[2] Sarvari, S. M. H., Howell, J. R., and Mansouri, S. H., "Inverse Boundary Design Conduction–Radiation Problem in Irregular Two-Dimensional Domains," *Numerical Heat Transfer*, Vol. 44, No. 3, 2003, pp. 209–224.
doi:10.1080/713836377

[3] Wu, C. Y., and Ou, N. R., "Transient Two-Dimensional Radiative and Conductive Heat Transfer in a Scattering Medium," *International*

*Journal of Heat and Mass Transfer*, Vol. 37, No. 19, 1994, pp. 2675–2686.
doi:10.1016/0017-9310(94)90384-0

[4] Yuen W. W., and Takara, E. E., "Analysis of Combined Conductive-Radiative Heat Transfer in a Two- Dimensional Rectangular Enclosure with a Gray Medium," *Journal of Heat Transfer*, Vol. 110, No. 2, 1988, pp. 468–474.
doi:10.1115/1.3250509

[5] Succi, S., *The Lattice Boltzmann Method for Fluid Dynamics and Beyond*, Oxford Univ. Press, Oxford, England, 2001.

[6] Mishra, S. C., and Roy, H. K., "Solving Transient Conduction and Radiation Heat Transfer Problems using the Lattice Boltzmann Method and the Finite Volume Method," *Journal of Computational Physics*, Vol. 223, No. 1, 2007, pp. 89–107.
doi:10.1016/j.jcp.2006.08.021

[7] Kim, K. W., Baek, S. W., Kim, M. Y., and Ryou, H. S., "Estimation of Emissivities in a Two-Dimensional Irregular Geometry by Inverse Radiation Analysis using Hybrid Genetic Algorithm," *Journal of Quantitative Spectroscopy and Radiative Transfer*, Vol. 87, No. 1, 2004, pp. 1–14.
doi:10.1016/j.jqsrt.2003.08.012

[8] Das, R., Mishra, S. C., Ajith, M., and Uppaluri, R., "An Inverse Analysis of a Transient 2-D Conduction–Radiation Problem using the Lattice Boltzmann Method and the Finite Volume Method Coupled with the Genetic Algorithm," *Journal of Quantitative Spectroscopy and Radiative Transfer*, Vol. 109, No. 11, 2008, pp. 2060–2077.
doi:10.1016/j.jqsrt.2008.01.011

[9] Moparthi, A., Das, R., Uppaluri, R., and Mishra, S. C., "Optimization of Heat Fluxes on the Heater and the Design Surfaces of a Radiating-Conducting Medium," *Numerical Heat Transfer*, Vol. 56, No. 10, 2009, pp. 846–860.
doi:10.1080/10407780903423841

[10] Mondal, B., and Mishra, S. C., "Analysis of 3-D Conduction-Radiation Heat Transfer using the Lattice Boltzmann Method," *Journal of Thermophysics and Heat Transfer*, Vol. 23, No. 1, 2009, pp. 210–215.
doi:10.2514/1.37948

[11] Mondal, B., and Mishra, S. C., "The Lattice Boltzmann Method and the Finite Volume Method Applied to Conduction-Radiation Problems with Heat Flux Boundary conditions," *International Journal for Numerical Methods in Engineering*, Vol. , No. , 2008.
doi:10.1002/nme.2482

[12] Mishra, S. C., Kumar T. B. P., and Mondal, B., "Lattice Boltzmann Method Applied to the Solution of Energy Equation of a Radiation and Non-Fourier Heat Conduction Problem," *Numerical Heat Transfer*, Vol. 54, No. 8, 2008, pp. 798–818.
doi:10.1080/10407780802424155